PAPER

High-cycle electromechanical aging of dielectric elastomer actuators with carbon-based electrodes

To cite this article: C A de Saint-Aubin *et al* 2018 *Smart Mater. Struct.* **27** 074002

View the article online for updates and enhancements.

Related content

- A survey on dielectric elastomer actuators for soft robots
  Guo-Ying Gu, Jian Zhu, Li-Min Zhu et al.

- Self-sensing dielectric elastomer actuators in closed-loop operation
  Samuel Rosset, Benjamin M O'Brien, Todd Gisby et al.

- Muscle-like high-stress dielectric elastomer actuators with oil capsules
  Thanh-Giang La, Gih-Keong Lau, Li-Lynn Shiau et al.

Recent citations

- Samuel Schlatter *et al*

High-cycle electromechanical aging of dielectric elastomer actuators with carbon-based electrodes

C A de Saint-Aubin[1], S Rosset[1,2], S Schlatter[1] and H Shea[1]

[1] Soft Transducers Laboratory (LMTS), École Polytechnique Fédérale de Lausanne (EPFL), Neuchâtel, Switzerland
[2] Biomimetics Laboratory, University of Auckland, New Zealand

E-mail: herbert.shea@epfl.ch

CrossMark

Abstract

We present high-cycle aging tests of dielectric elastomer actuators (DEAs) based on silicone elastomers, reporting on the time-evolution of actuation strain and of electrode resistance over millions of cycles. We compare several types of carbon-based electrodes, and for the first time show how the choice of electrode has a dramatic influence on DEA aging. An expanding circle DEA configuration is used, consisting of a commercial silicone membrane with the following electrodes: commercial carbon grease applied manually, solvent-diluted carbon grease applied by stamping (pad printing), loose carbon black powder applied manually, carbon black powder suspension applied by inkjet-printing, and conductive silicone-carbon composite applied by stamping. The silicone-based DEAs with manually applied carbon grease electrodes show the shortest lifetime of less than 10^5 cycles at 5% strain, while the inkjet-printed carbon powder and the stamped silicone-carbon composite make for the most reliable devices, with lifetimes greater than 10^7 cycles at 5% strain. These results are valid for the specific dielectric and electrode configurations that were tested: using other dielectrics or electrode formulations would lead to different lifetimes and failure modes. We find that aging (as seen in the change in resistance and in actuation strain versus cycle number) is independent of the actuation frequency from 10 Hz to 200 Hz, and depends on the total accumulated time the DEA spends in an actuated state.

Supplementary material for this article is available online

Keywords: DEA, stretchable electrode, aging, carbon

(Some figures may appear in colour only in the online journal)

1. Introduction

Dielectric elastomer actuators (DEAs) are soft transducers consisting of an electrically insulating elastomer membrane sandwiched between two compliant electrodes. When used as an actuator, applying a voltage between the two electrodes leads to an electrostatic force that squeezes the membrane, causing it to expand in-plane. The working principle of DEAs was documented in key publications of the late 1990's [1, 2]. Since then, DEAs have been investigated for a wide range of applications such as haptic interfaces, tunable optics, soft-robotics, sensors, microfluidics and biomedical devices [3–7].

The interest in the technology was primarily due to the high actuation strains that DEAs can achieve; in 2011 a snap-through configuration leading to area strain of 1692% was reported [8].

A number of DEA-based devices have been commercialized, such as the haptic devices and headphones by Vivitouch [9] and the laser speckle reducer by Optotune [10]. More information on the aging of DEAs is required to apply DEAs to new application fields.

In the present work, data on aging of the electrodes used for DEAs is presented for the first time. DEAs were actuated electromechanically to reproduce the real operating

conditions. We compare DEAs made with the same silicone membrane but with carbon-based compliant electrodes of different compositions and/or application methods. We find that the time evolution of the resistance of the electrodes and DEA performance is strongly dependent on the choice of materials (elastomer and electrode) and the electrode application method. We also study the impact of actuation frequency on the high-cycle aging of a DEA. We find that the degradation of the electrodes and stretching performance of the DEA do not directly depend on the number of stretching cycles, but rather on the total time the DEA is kept in its stretched state.

To study the aging of DEA electrodes, we developed an automated system called the Novel Electrode Resistance Degradation (NERD) setup, see Rosset *et al* for a complete description [11]. The NERD setup, described in section 2.1, monitors the resistance and stretch of a DEA with a circular electrode. A high-voltage power supply drives the actuator with a square wave to periodically stretch the electrodes. Previous aging studies have used mechanical setups to stretch the electrode uniaxially. In contrast, the NERD setup monitors the aging of DEAs under more realistic equibiaxial stretch. In Rosset *et al*, we used the NERD setup to characterize carbon-black/silicone composite commonly used in our laboratory as a compliant electrode [12]. This composite is well-suited for tens of millions of actuation cycles at 5% strain. However, at 20% in-plane strain, the electrodes degrade after a few thousand cycles.

Very few studies of have investigated aging of DEAs over many cycles. York and co-workers published low-cycle ($n < 10^3$) fatigue tests on pressure sensors [7]. They observed a drift in the performance of the devices after 500 loading-unloading cycles. The drift is attributed to the electrode layer deterioration, causing a decrease in the effective capacitance. Matysek and co-workers studied the aging of stacked DEAs based on an Elastosil P7670 (Wacker Chemie) silicone-membrane, over 320×10^6 cycles of contraction-expansion of the stack [13]. Failures were due to the interconnections between electrode layers. This result points out an important technological issue stemming from stacking DEAs but it does not provide insights on the fundamental aging issues that can emerge from the choice of materials. Haruna and co-workers published a study showing the gradual increase in displacement of an expanding circle actuator based on the acrylic VHB 4910J (3M) membrane over 10^5 cycles [14]. Creep of the highly viscous VHB membrane was found to be the cause of the degradation. Finally, Zhang and co-worker published studies on mechanical and electromechanical aging of DEAs based on DMS-V33/HMS-151 (Gelest Inc.) silicone membranes [15]. Over 10^5 loading-unloading cycles the crosslink density in the polymer was found to increase. As a consequence, the elastic modulus of the polymer increases, the electric permittivity decreases, and the breakdown strength increases. While these results show the deterioration of a DEA membrane, the evolution of the actuation deformation over aging was not measured, but rather modelled. Furthermore, the simple DEA model that was used did not include the mechanical effect of the electrodes.

In this paper, we provide quantitative aging results using the NERD setup [11] to monitor high-cycle ($n > 10^6$) electro-mechanical aging of DEAs based on silicone membranes. In section 2, we describe the methods used to measure high-cycle electro-mechanical aging of DEA electrodes and the methods used to fabricate the DEAs. In section 3, we present the results of the high-cycle aging tests of DEAs based on a silicone membrane with electrodes of different composition and/or application methods. The different compositions/application methods are: Nyogel carbon grease applied manually through a mask, solvent diluted carbon grease applied by stamping (pad-printing), loose carbon black powder applied manually through a mask, carbon black powder suspended in a solvent with a surfactant applied by inkjet printing, and conductive rubber applied by stamping (pad-printing). Finally, we describe the impact of the actuation frequency on aging.

2. Measurement setup and device fabrication

2.1. Measurement of electrode degradation with the NERD setup

We use a custom setup, the NERD setup, to measure high cycle aging of DEAs. In brief, the NERD setup monitors simultaneously the linear stretch (in-plane stretch) and the electrode resistance of an expanding circle actuator (active area of approx. 10 mm^2) as a function of cycle number and drive voltage. The NERD setup uses optocouplers to generate a high-voltage and high-frequency square wave, making it possible to test DEAs fairly rapidly over millions of cycles. The NERD setup is described in detail in [11].

A square drive voltage with a frequency of 50 Hz is used, with an amplitude of V_{test} chosen to avoid the electrical breakdown of the DEA. The actuation profile is shown in figure 1. Every 2000 cycles, after one cyclic actuation block, the linear stretch and electrode resistance at 0 V and at V_{test} are measured in what is called the acquisition cycle. For each measurement the voltage is held constant for 5 s to allow the sample to stabilize. Every 50 000 cycles, a voltage ramp is applied where the linear stretch and electrode resistance are measured at 8 voltage levels between 0 V and at V_{test}. Again, the voltage is held constant for 5 s before taking the measurement. This voltage ramp makes it possible to plot stretch versus voltage and resistance versus stretch every 50 000 cycles, to evaluate the degradation of the device.

The devices are tested over millions of cycles to emulate the conditions encountered by devices in industrial settings. To limit the tests to a reasonable timespan, the test was conducted at 50 Hz. At this frequency, the tests can be conducted in a number of hours and the actuator reaches stretch values close to the stretch at DC conditions (0.1 Hz). The square waveform mimics the harshest conditions by imposing a very high stretch rate (dV/dt) on the actuator. If a DEA survives this worst-case scenario, it will most probably survive milder aging conditions as well. The drive voltage is applied to the actuator using an in-house compact

Acquisition cycle: **measure <u>R</u> and linear <u>strain</u>** at V=0 and at V=V$_{test}$
Cyclic actuation: cycle through fast actuation to quickly accumulate actuation cycles (50 Hz)
Voltage ramp: ramp up voltage and **measure <u>R</u> and linear <u>strain</u>** vs. voltage, every 50,000 cycles.
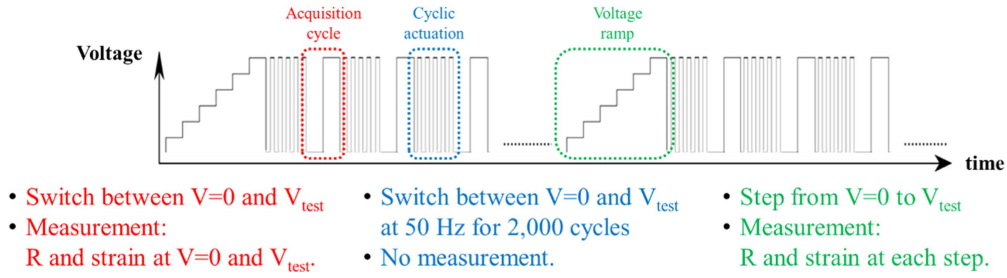

- Switch between V=0 and V$_{test}$
- Measurement:
  R and strain at V=0 and V$_{test}$.

- Switch between V=0 and V$_{test}$
  at 50 Hz for 2,000 cycles
- No measurement.

- Step from V=0 to V$_{test}$
- Measurement:
  R and strain at each step.

Figure 1. The three different blocks of a NERD test: the acquisition cycle block, the cyclic actuation block, and the voltage ramp block. For each measurement the voltage is held constant for 5 s to allow the sample to stabilize.
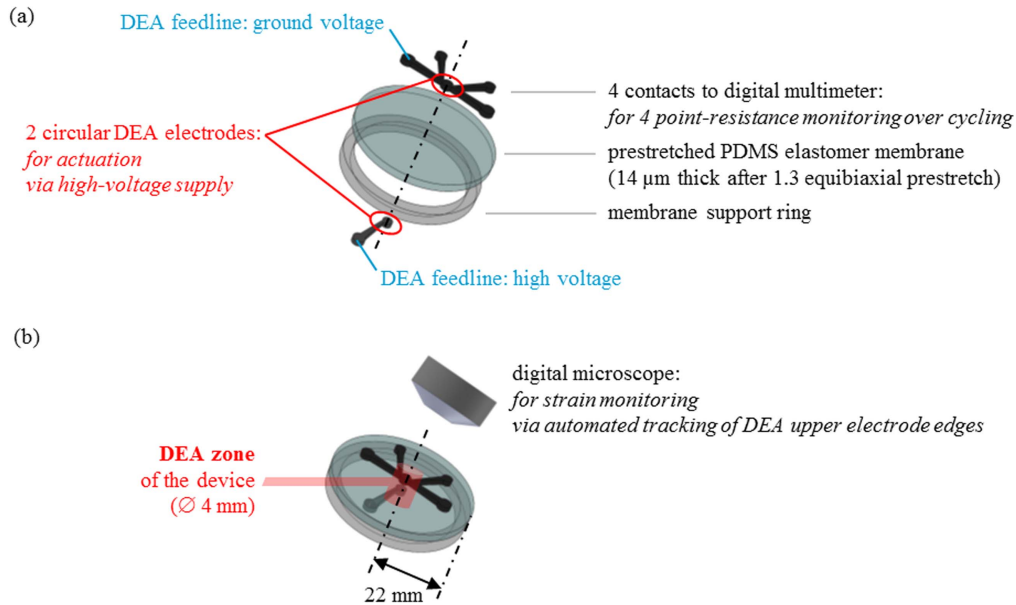

Figure 2. (a) Exploded view of a NERD DEA device. (b) Compact view of the device. The conductive and compliant material composing the top and bottom patterns applied on the PDMS elastomer membrane is represented in black.

programmable high voltage supply [16]. The deformation of the DEA is recorded with a digital microscope and the linear stretch is calculated from the diameter change of the active zone when actuated.

The devices for the NERD setup are depicted in figure 2. The top and bottom electrodes are applied on a 1.3 equibiaxially prestretched membrane (14 μm thick after prestretch), fixed onto a 22 mm diameter support ring. The top electrode consists of a circle (4 mm diameter) and four contacts to measure the 4-point resistance of the electrode. The top electrode is at a low potential. The bottom electrode has a single contact and is at a high potential.

2.2. Choice of materials for the membrane and electrodes of the DEAs

A silicone elastomer is used for the membrane. The electrodes are based on carbon. The aging processes we observe are strongly dependent on the electrode-dielectric interactions. Other electrode formulations could lead to very different

lifetimes. However, our method is general, and could be used directly on DEAs made with polyurethane, acrylics, natural rubber or other elastomers.

All the devices tested in this paper were made from a commercial 20 μm-thick Wacker Elastosil 2030 polydimethylsiloxane (PDMS) membrane. Silicone membranes have a long lifetime and short response time when used in DEAs, [11] and are therefore well suited for commercial devices. In the DEA literature, a commercial acrylic adhesive, VHB from 3 M, is often used because very large strains are attainable. However, VHB actuators have a long response time due to the material's high viscoelasticity [4]. In addition VHB-based devices generally have low and unpredictable lifetime due to crack propagation in the highly pre-stretched films. VHB-based devices therefore are not a suitable option for most commercial applications. [11, 17]. Moreover, using a commercial membrane (as opposed to casting the membrane ourselves from liquid silicone components) allows us to have a stable reference (constant membrane thickness and stiffness). The differences observed between devices using
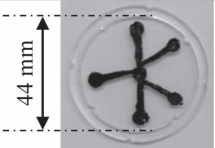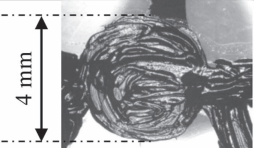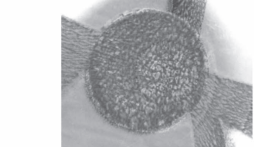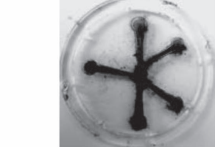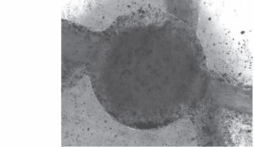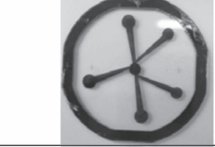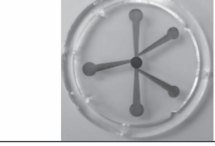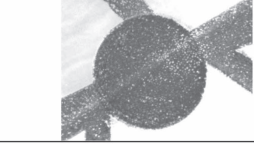
Figure 3. Pictures of the tested DEAs with electrodes of different compositions and/or application methods: global device view (left) and zoom onto the DEA electrode (right).

different electrode types can therefore be attributed solely to the change in electrode type.

The most widely used electrodes within the DEA community [18–22] are loose carbon powder, carbon grease and conductive rubber, for cost, ease of patterning, low mechanical stiffening, and lifetime reasons. A very wide range of compliant electrodes have been used for DEAs, as reviewed in [20] and [22]. Beyond carbon-based solutions, there are many other interesting options such as ionogels, hydrogels swelled with a salt solution, liquid metals, and conductive polymers [20]. For this study, we opted to use only those carbon-based electrodes because this already led to 5 different combinations of materials and printing methods, and because carbon-based electrodes are the most widely used and the most mature.

2.3. Fabrication of the devices

Three types of electrode patterning methods were used to fabricate the devices: hand-application through a mask, stamping (pad-printing) and inkjet-printing. Figure 3 summarizes the materials and patterning methods that were used.

The devices made with loose carbon powder were made with Ketjenblack EC-300J (AkzoNobel). A mask was made from an overhead transparency coated with a thin layer of

cured silicone; the cured silicone improves mask adhesion on the silicone membrane. The electrode designs were cut out with a laser cutter. Carbon powder was also applied by inkjet printing. For these samples, the carbon black (Ketjenblack EC-300J) was dispersed in a solvent with the help of a surfactant (Belsil SPG 128 VP from Wacker Chemie) according to the procedure described in Schlatter *et al* [23]. Carbon grease samples were produced either by applying the pure carbon grease Nyogel 756G (Nye Lubricants) onto the silicone membrane through a mask, or by stamping (pad printing) a mixture of carbon grease diluted with a solvent. The devices composed of a conductive rubber were produced according to the procedure described in [12]. Carbon black (Ketjenblack EC-600JD from AkzoNobel) and a silicone elastomer (Silbione LSR 4305 from Bluestar Silicones) are mixed together in a planetary mixer, diluted in a solvent, and patterned on the prestretched membrane by pad-printing (an automated stamping method).

2.4. Evaluation of fabrication methods

Images of the patterned electrodes are shown in figure 3. The electrodes were most precisely defined by stamping and inkjet printing. The electrodes produced with those patterning techniques have cleaner edges, better thickness homogeneity,

and better front-to-back alignment than the samples with electrodes manually applied through a mask. When carbon grease is smeared onto a membrane, the pattern reproduction is very poor. The thickness of the grease/manual electrode is of the order of 100 μm and it is difficult to replicate the electrode design accurately. We improved the patterning of carbon grease onto the silicone membrane by diluting it with a solvent and stamping it to pattern the electrodes. With this approach, the electrode pattern is better reproduced and the electrode is thinner and more uniform (1–2 μm with a roughness of $\sim$0.5 μm). A poorly resolved pattern is obtained when loose carbon black powder is manually applied through a mask. Electrostatic charging of the powder causes the powder to spread when the mask is removed. Using inkjet printing leads to much better results. With inkjet printing we obtained clearly resolved patterns with thicknesses down to 0.3 μm. Stamped conductive rubber electrodes also produced well defined electrodes. We obtained electrodes with thicknesses down to 0.5 μm.

3. Results and discussion

3.1. Influence of the electrode on the device high-cycle aging

In this section we present the results of the high cycle aging tests and discuss how the different electrode materials have a pronounced effect on the aging behaviour of DEAs. We emphasize that our results are valid only for the material combinations used here, and cannot be taken as general trends for DEAs made using other elastomers or other electrode formulations.

This section is split into four subsections. Section 3.1.1 presents the results in a tabular format showing how the resistance and stretch have changed between cycle 1 and cycle 10^6. The table also shows the proportion of devices which failed before 10^6 cycles and gives the maximum number of cycles reached if breakdown did not occur. In the section 3.1.2, typical curves are plotted to show how the resistance and stretch of devices evolve as a function of cycle number. Finally, in sections 3.1.3 and 3.1.4, the stretch and resistance aging curves are discussed in detail and the observed behaviours are interpreted.

3.1.1. Summary of test results.
A summary of the results is given in table 1. The first column of the table indicates the type of material and the method used to pattern the electrode. For each type, we tested numerous devices. Each device was submitted to a 10^6 cycle NERD test. The actuation voltage V_{test} was set to achieve an initial linear strain of 5%. A strain of 5% was chosen to avoid electrical breakdown during the test; generally, silicone-based DEAs break down at linear strains below 20%. The second column of the table gives the proportion of devices that failed before the end of the test. The third, fourth, and fifth columns give the percentage change in resistances and the final strain after 10^6 cycles. The resistance is given in the unactuated (V = 0 V) and actuated (V = V_{test}) states. The strain is only given for the actuated

state (V = V_{test}). The values in columns three and four were calculated by averaging all the measurements of the devices surviving one million cycles.

The last column indicates the lifetime of the different devices. For the devices which failed before 10^6 cycles we display the cycle number at failure. For devices that function after one million cycles, we show the cycle number with a > sign, as these devices continued to function but the testing was stopped at the given cycle number. The tests which exceeded 10^6 cycles were over successive NERD tests which were interrupted once or many times. The cumulated number of cycles is given in the last column of the table. Please note that these lifetime values are merely an indication of the lifetime. The dielectric breakdown of a DEA is a stochastic phenomenon; at least 20–25 samples should be tested to estimate lifetime [13, 24].

The electrodes based on the commercial carbon-grease, regardless of the application method, break down the earliest. From table 1, we see that some devices operate for thousands or tens of thousands of cycles and others operate for millions of cycles. For the devices that operated for 10^6 or more cycles, the resistance of the electrode remains stable and changes by less than 10% over 10^6 cycles. The linear stretch after 10^6 cycles increases to 5.5%. On the contrary, DEAs based on powder/manual, powder/inkjet and rubber/stamping electrodes, all continued to operate after 10^6 cycles. However, the electrode resistance increases more substantially than carbon grease electrodes. For DEAs based on powder/manual and on powder/inkjet electrodes, the resistances increased by 300%. For rubber/stamping electrodes, the resistances less than doubled with high-cycle aging. The strain of these devices degraded slightly to 4% after one million cycles. Aging tests have been carried out on more than one hundred DEAs based on rubber/stamping electrodes but with different electrode rubber formulations. Despite the formulation changes, all these DEAs survived the one million cycle NERD test without failure. The robustness of DEAs based on rubber/stamping electrodes goes well beyond the case of the single formulation detailed in the present paper.

For the devices based on powder/manual, powder/inkjet or rubber/stamping electrodes, we extended the tests beyond 10^6 cycles. One DEA with powder/manual electrodes sustained 14.10^6 cycles, as did a DEA with powder/inkjet electrodes, and a DEA with rubber/stamping electrodes sustained 41.10^6 cycles. Note that these figures represent the cycle number when the test was halted. It is very likely that these devices would continue to operate if the tests were continued.

The table shows that our DEAs with carbon grease electrodes are not reliable. On the contrary, DEAs made with powder/manual, powder/inkjet and rubber/stamping electrodes are capable of sustaining tens of millions of cycles without failing. There is some loss in performance, resistance drift and reduced stretch, but this is preferred over catastrophic failure. Considering the ease and quality of electrode patterning with inkjet printing and stamping, it can be stated that powder/inkjet and rubber/stamping electrodes make reliable and robust devices.

Table 1. Comparison of the performance during high-cycle aging tests of DEAs made with electrodes of different compositions and/or application methods. The maximum strains for the DEAs are 11%–15% linear strain. The amplitude V_{test} of the square actuation voltage of a frequency of 50 Hz was chosen for each device so as to impose an initial linear strain of 5%.

Electrode type	Number of DEAs that	Change in R at 0 V	Change in R at V_{test}	Linear strain at V_{test} after 10^6	Lifetime (# of
Initial linear strain at V_{test} (average V_{test})	failed before 10^6 cycles	after 10^6 cycles (%)	after 10^6 cycles (%)	cycles (%)	cycles)
Grease/Manual 5% (930 V)	2 of 2		DEA failure		62000 and 88000
Grease/Stamping 5% (980 V)	5 of 11	+6%	+3%	5.5	6,000 to $>11.10^6$
Powder/Manual 5% (970 V)	0 of 2	+330%	+280%	4	$>14.10^6$
Powder/Inkjet 5% (940 V)	0 of 4	+340%	+160%	4	$>14.10^6$
Rubber/Stamping 5% (990 V)	0 of 7	+76%	+70%	4	$>41.10^6$

3.1.2. Typical results: resistance and linear stretch aging curves. In this section, we present high-cycle aging curves that are typical of the different electrode compositions and/or application methods (figure 4). These curves show the effects of high-cycle aging on the linear stretch (figure 4(a)) and on the resistance (figure 4(b)) of the tested devices.

Figure 4(a) plots $\lambda_{V0,n}$ and $\lambda_{Vtest,n}$ versus cycle number. The linear stretch in the non-actuated state is given at cycle n by [3] $\lambda_{V0,n} = \frac{r_{V0,n}}{r_{V0,0}}$, and the linear stretch when actuated at cycle n is given by $\lambda_{V_{test},n} = \frac{r_{V_{test},n}}{r_{V0,0}}$. Both are calculated with respect to the reference radius $r_{V0,0}$ taken at 0 V, cycle zero. Figure 4(b) shows how the electrode resistance at 0 V $R_{V0,n}$ and at V_{test} $R_{V_{test},n}$ evolve with increasing cycle number n. All experiments were conducted on the NERD setup at a frequency of 50 Hz and with an actuation voltage V_{test} to give an initial actuation of 5% linear strain.

The different electrode compositions/application methods lead to different behaviours. The plots in figure 4 are for one representative sample of each DEA preparation method.

3.1.3. Discussion on the stretch aging-curves. In this part, we discuss the linear stretch curves (figure 4(a)) and propose explanations for the observations.

The powder/manual, powder/inkjet, and rubber/stamping electrode DEAs all show versus cycle number a slight increase of linear stretch at 0 V and a slight decrease in linear

stretch at V_{test}. The rate at which $\lambda_{V0,n}$ increases was higher during the first 200 000 cycles. We attribute this principally to creep of the membrane, as no significant differences were observed between the three different electrode compositions. Creep is the slow progressive deformation of a sample submitted to a constant load and is related to the viscous nature of a material. Creep is often described as delayed elasticity because it is the non-immediate response of the material to a load change [25]. If the load is periodic, creep accumulates at every cycle if the time for recovery is higher than the period of the signal. This has been shown by Haruna *et al* [14] observed on DEAs with highly viscoelastic VHB4910J membranes. Cumulative creep is also present in our experiments: each time we subjected a sample to a new NERD test, whether fresh or previously tested (allowed to rest for a few hours), the linear stretch at rest $\lambda_{V0,n}$ increased rapidly at the beginning of the experiment and leveled off as the cycle number increased.

Permanent set could also have had an influence on the evolution of $\lambda_{V0,n}$. It is a non-elastic phenomenon typical of elastomers: stretched elastomers do not return to their initial position after load release but hold a residual deformation even after a long rest [26, 27]. The typical profile of a permanent set curve over aging is an increase followed by a plateau. Permanent set is not demonstrated through our NERD tests, as it lies within our experimental uncertainty. We mention permanent set in a general perspective, as it could play a role for other types of membranes.

To better understand the decrease of $\lambda_{V_{test},n}$ in figure 4(a) we performed interrupted NERD tests on a rubber/stamping

---

[3] $X_{V,n}$ represents the value of a quantity X at the voltage V at cycle number n. For instance, $r_{V0,0}$ represents the radius in pixels of the electrode at 0 V at cycle 0.
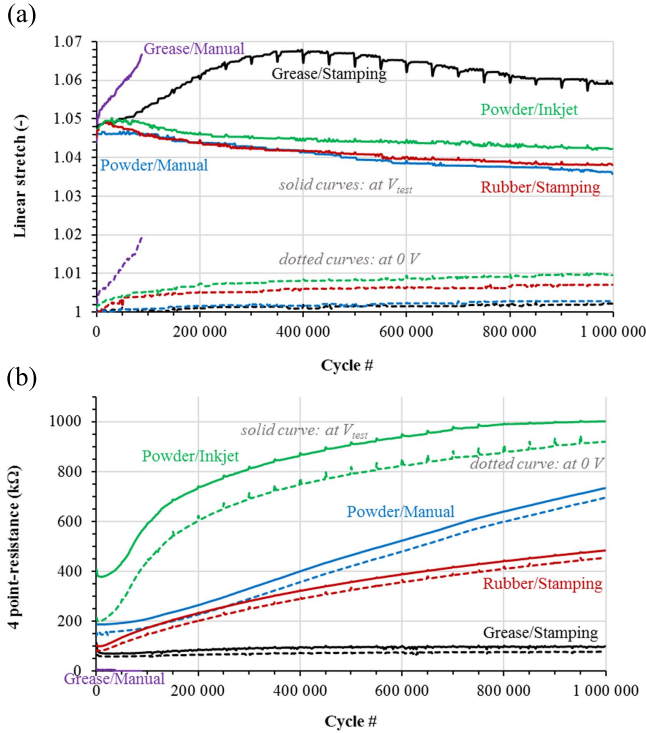
(a)

(b)

Figure 4. Aging of representative DEAs with different electrodes up to 10^6 cycles: (a) linear stretch referenced to the electrode radius at cycle 0 versus cycle number. Dotted curves: stretch $\lambda_{V0,n}$ at 0 V; solid curves: stretch $\lambda_{V_{test},n}$ at the voltage V_{test} (b) 4 point-resistance versus cycle number. Dotted curves: $R_{V0,n}$ at 0 V; solid curves: $R_{V_{test},n}$ at the voltage V_{test}. An initial stretch of 1.05 was imposed at cycle 0 by applying a constant voltage V_{test}, different for each sample. The spikes on the curves every 50 000 cycles are measurement artefacts due to the measurement of the full ramp every 50 000 cycles (see [11] for more explanations).
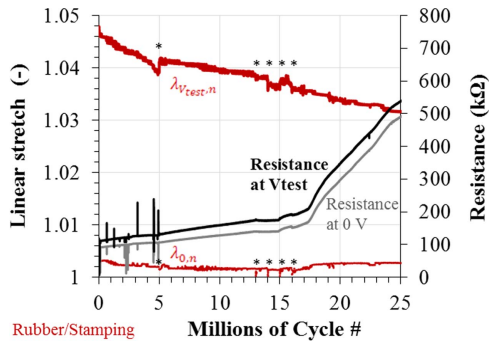

Figure 5. Linear stretch $\lambda_{V0,n}$ and $\lambda_{V_{test},n}$ versus cycle number (left axis, red curves) and 4 point-resistance $R_{V0,n}$ and $R_{V_{test},n}$ (right axis, grey curves). DEA based on rubber/stamping electrodes. The stars indicate resting periods of 32 h, 2 h, 30 min, 5 h and 40 h.

device. The interruptions ranged from 30 min to 32 h. Throughout the tests, V_{test} was kept constant. Figure 5 plots the linear stretch $\lambda_{V0,n}$ and $\lambda_{V_{test},n}$ as a function of cycle number for a DEA with rubber/stamping electrodes. The plot shows that the rest periods do not allow the device to recover to the initial linear stretch $\lambda_{V_{test},0}$. Following a rest period, the linear stretch $\lambda_{V_{test},n}$ is approximately the same as before the

rest period. Hence, the observed decrease of $\lambda_{V_{test},n}$ cannot be due to instantaneous elasticity, nor to delayed elasticity with a time constant of hours or days [26, 28]. The decrease of $\lambda_{V_{test},n}$, and hence the aging of the device, is irreversible.

The decrease of $\lambda_{V_{test},n}$ can only stem from the increased stiffness of the elastomer and/or a decrease of the electro-static actuation force (e.g. decrease in elastomer permittivity of the degraded membrane). Stiffening of the elastomer membrane would affect both $\lambda_{V_{test},n}$ and $\lambda_{V0,n}$ which is not the case. The observed decrease of $\lambda_{V_{test},n}$ must therefore be due to a change in permittivity and/or the resistivity of the membrane.

The DEAs based on grease/manual electrodes showed a strong linear increase in $\lambda_{V0,n}$ and $\lambda_{V_{test},n}$ (figure 4(a)). The rapid increase of $\lambda_{V0,n}$ in grease/manual devices was far more pronounced than for powder or carbon-PDMS composite devices. Although creep is likely to be a culprit, creep alone cannot explain the difference. The mostly likely cause for the increase is a softening of the membrane. The softening can be attributed to the oil in the carbon grease electrodes. Nyogel 756 G carbon grease is composed of carbon black and a liquid polyalphaolefin ('Synthetic oil 181'). The oil can separate from the carbon over time and penetrate into the PDMS membrane. Indeed, after six months, the entire membrane of these devices has a yellow tint –the tint of the oil–, a phenomenon not observed on devices with different electrode types. The affinity between the polyalphaolefin oil of the carbon grease and the PDMS of the membrane is supported by two facts. First, polyalphaolefins oils and silicone oils are miscible at room temperature [29]. Second, hydrocarbons like heptane (chemically close to polyalphaolefins), swell PDMS to a high degree [30]. The degradation of a DEA due to the diffusion of a liquid from the electrode into the membrane has previously been suggested by Buchberger *et al* [31].

If carbon grease electrodes were prepared using an oil that does not swell silicones, the lifetime of such silicone-based DEAs would greatly improve. We did not test this as we could not obtain a commercially available non-swelling grease for silicones. However, reliable silicone-based DEAs using carbon grease electrodes have been reported by Fasolt *et al*, using the Wacker AK 100 K silicone oil [32].

Performance of DEAs using grease electrodes would also clearly be improved by using dielectrics that do not swell when exposed to carbon grease. VHB is an example of such an elastomer, for which carbon grease could be a suitable electrode.

Grease/stamping DEAs showed a very different linear stretch evolution than grease/manual DEAs. The linear stretch $\lambda_{V0,n}$ increased only slightly, and $\lambda_{V_{test},n}$ has a maximum around 400 000 cycles (figure 4(a)). The samll increase in $\lambda_{V0,n}$ was similar to the evolution we have seen in powder or carbon-PDMS composite devices. It is likely that this behaviour can also be attributed to creep and permanent set. The presence of a maximum in the $\lambda_{V_{test},n}$ curve is an indication of two antagonistic aging processes, one leading to higher strains (dominating below approximately 4.10^5 cycles) and one to lower strains (dominating above approximately 4.10^5 cycles). The origin of the increase in $\lambda_{V_{test},n}$ is probably

the same as for the grease/manual devices (membrane softening due to the diffusion of carbon grease oil). The decrease of $\lambda_{V_{test},n}$ after 4.10^5 cycles may be explained by the same by reasoning as for powder or carbon-PDMS composite devices (reduced actuation due to a decrease in membrane permittivity). Hence, grease/stamping electrodes appear to be a combination of the other two behaviours. For grease/stamping devices we did not observe any yellowing of the membrane after several months. Since the grease/stamping electrodes are about 100 times thinner than grease/manual electrodes, they contain significantly smaller amounts of oil. A reduction of this specific carbon grease oil amount means less swelling and softening of the membrane, ultimately leading to more reliable devices and less failure.

3.1.4. Discussion on the resistance aging-curves.

In this part, we discuss the 4-point resistance curves in figure 4(b) and propose explanations for the observations. Figure 4(b) shows the change in resistance due to actuation and the evolution of the resistance due to cycling.

The change in resistance due to actuation (i.e. the difference between the dashed and the solid curves in figure 4(b)) was measureable for all except grease/manual devices. We attribute this to the more fluid nature of the thick grease/manual electrodes. When those electrodes were stretched, the conductive particles could rearrange, thanks to the mobility provided by the oil. When less or no oil is present, the mobility is reduced and a change in resistance is observed. For powder and rubber/stamping devices, 4 point-resistance was higher in the stretched state than in the unstretched state. We have shown in Rosset *et al* that 4 point-resistance in the NERD setup is directly linked to electrode sheet resistance R_{square}. [11] Because $R_{square} = 1/(\sigma t)$ (σ: conductivity of electrode material; t: thickness of electrode), an increase of the NERD 4 point-resistance with stretching indicates a decrease of σt during stretching. A decrease of the intrinsic conductivity σ with stretching is due to changes in the interconnectivity of the conducting zones in the electrode and depends on the nature of the conducting media. For instance, in gold electrodes the changes stem from micro-cracks [33]. A decrease of the thickness t with stretching occurs if the electrode is made of a continuous, compliant but non fluid material like conductive rubber; it is less likely with more liquid like electrodes such as carbon grease.

In terms of the evolution of resistance due to cycling, the powder and rubber/stamping electrodes showed a clear increase in resistance with cycle number, whereas grease electrodes did not. Resistance of powder and rubber/stamping electrodes increased by a factor of 5 after a 10^6 cycles. The increase in resistance can be attributed to damage of the conducting network in the electrodes. The damage is irreversible, as was demonstrated in the interrupted NERD tests (figure 5). The figure also shows a steeper increase in resistance near 18.10^6 cycles where the degradation becomes more severe. The test showed that the rate of aging is not fixed with cycle number. It is therefore necessary to test devices for the complete number of cycles that a device will
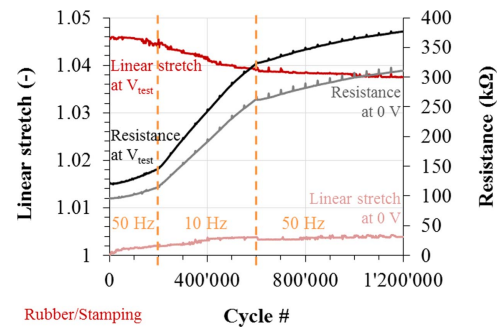

Figure 6. Effect of varying the drive frequency: 50 Hz, then 10 Hz, then 50 Hz from cycle 0/ 200,000/ 600,000. Linear stretch $\lambda_{V0,n}$ at 0 V and linear stretch $\lambda_{V_{test},n}$ at V_{test} ($V_{test} = 986$ V) versus cycle number (left axis); 4 point-resistance $R_{V0,n}$ at 0 V and $R_{V_{test},n}$ at V_{test} versus cycle number (right axis). DEA based on rubber/stamping electrodes.

ultimately endure. Devices based on grease/manual electrodes showed remarkably stable resistances over their short lifetime. This is attributed to the rearrangement of the conducting network as was discussed earlier.

3.2. Influence of actuation frequency on high-cycle aging

It has been shown that the lifetime of elastomers under fatigue depends on the frequency of the periodic mechanical load. High frequency loading leads to heating of the elastomer (due to viscoelasticity) and the heating leads to accelerated aging. Elastomers under high frequency loading therefore can have a shorter lifetime [34], if the high frequency loading leads to heating. Given the very low power required to drive a DEA, such heating may not be significant for DEAs. We thus investigated whether actuation frequency has an impact on the high-cycle aging of DEAs. The experiment was conducted on a device with rubber/stamping electrodes. The device was actuated at 986 V. The frequency was set to 50 Hz between cycle zero and cycle 200 000, then reduced to 10 Hz from cycle 200 000 to cycle 600 000, and increased to 50 Hz from cycle 600 000 to cycle 1200 000. We plot the resistance and stretch curves as a function of two different aging parameters: (i) number of cycles, and (ii) cumulative time in the actuated state. The interpretation of the data is different depending on the choice of the aging parameter.

Figure 6 shows the results of the experiment expressed as a function of the number of cycles, the usual aging parameter. The linear stretch $\lambda_{V0,n}$ increases more rapidly during 10 Hz cycling phase. This shows that creep accumulation per cycle is higher at lower frequencies, a phenomenon also described by Haruna *et al* [14]. Similarly, the linear stretch $\lambda_{V_{test},n}$ decreases more rapidly during the 10 Hz cycling phase. The resistance of the electrode appears to also be affected by frequency. Both $R_{V0,n}$ and $R_{V_{test},n}$ increase more rapidly during the 10 Hz cycling phase. Hence, if we plot the performance of the DEA versus the cycle number, it appears to degrade more slowly at high frequency. This result remains valid if the frequency sequence is inverted from high-low-high to low-high-low; the corresponding data is shown in the
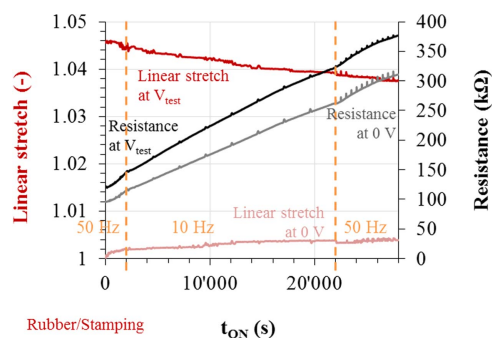
Figure 7. Effect of varying the drive frequency: 50 Hz, then 10 Hz, then 50 Hz from cycle 0/ 200,000/ 600,000. Linear stretch $\lambda_{V0,n}$ at 0 V and linear stretch $\lambda_{V_{test},n}$ at V_{test} ($V_{test} = 986$ V) versus t_{ON} of the square actuation voltage (left axis); 4 point-resistance $R_{V0,n}$ at 0 V and $R_{V_{test},n}$ at V_{test} versus t_{ON} of the square actuation voltage (right axis). DEA based on rubber/stamping electrodes.

supplementary data section S1 is available online at stacks.iop.org/SMS/27/074002/mmedia.

To ensure that the linear stretch data is valid at all testing frequencies, we conducted an experiment to determine the linear stretch as a function of frequency. The linear stretch was measured with a stroboscopic method [11] between 0.1 Hz and 1 kHz while V_{test} was held constant. The results obtained for rubber/stamping electrodes are given in the supplementary data S2. Starting from 0.1 Hz, we found that the linear stretch reduces by less than 10% at 50 Hz. The slower decrease of $\lambda_{V_{test},n}$ at high frequency in figure 6 is therefore due to slower aging and not to any limitation of the stretch effectively reached.

In figure 7, we plot the results of the same experiment as in figure 6, but we plot stretch and resistance as a function of the time the DEA is in the stretched state, t_{ON} (the very short transition time between 0 V and V_{test} is neglected). When presenting the data in this fashion, the linear stretch $\lambda_{V_{test},n}$ is a straight line which shows that frequency does not impact the aging curves. The same result was obtained for the low-high-low case (supplementary data, S3) and for the case were the frequency was changed between 10 and 100 Hz (supplementary data, S4). We have also observed this in similar experiments with powder/manual electrodes (supplementary data, S5 and S6).

These experiments show that the aging of DEAs is not due to heating of the elastomer. The viscoelasticity of the silicone membrane used in these experiments is low enough to avoid excessive heat generation during cyclic actuation. The fatigue of a DEA is caused by mechanical mechanisms, not thermal ones.

To summarise, the aging of a DEA can be defined in two ways. When aging is defined in terms of the number of cycles, it can be said that a DEA ages faster at low frequencies. However if aging is defined in terms of the cumulative actuated time, then aging is independent of the actuation frequency.

4. Conclusion

In this study, we have for the first time described how the choice of electrode composition and application method has a very large impact on the high-cycle electromechanical aging of silicone-based DEAs. The methodology used can be extended to DEAs made using other dielectric membranes and electrode formulations. The results we report are for specific combinations of electrode material and silicone membrane.

By using the NERD setup, we were able to cycle DEAs electromechanically for up to 40 million cycles at 50 Hz. We chose to operate at 5% strain because this was relatively near the breakdown electric field for the DEA configuration we used, and because it allowed using the same strain level for all electrode types we compared.

The DEAs with manually applied carbon grease electrodes (as is commonly done for VHB-based DEAs) showed the shortest lifetime: less than 10^5 cycles. Commercially-available carbon grease electrodes are convenient for quick and dirty low-cycle tests, especially on VHB membranes, but are unsuitable for making reliable silicone-based devices.

Inkjet-printed carbon powder and stamped silicone-carbon composite electrodes made for the most reliable silicone-based DEAs that we tested, with lifetimes greater than 10^7 cycles. In many cases, we stopped testing before the DEAs failed.

The degradation of the DEA stretch performance has two consequences. First, the actuated stretch amplitude of the DEA decreases. Second, the absolute rest position of the DEA increases due to creep and permanent set. We have shown that, if the material chosen for the membrane is not too viscoelastic, aging of the DEAs is independent of the actuation frequency. Aging depends on the total accumulated time in the actuated state.

Our results are of immediate practical use for making more robust DEAs, and pave the way for more fundamental studies in the physics of the degradation mechanisms.

ORCID iDs

H Shea ⬤ https://orcid.org/0000-0003-3527-3036

References

[1] Pelrine R E, Kornbluh R D and Joseph J P 1998 Electrostriction of polymer dielectrics with compliant electrodes as a means of actuation *Sens. Actuators Phys.* **64** 77–85

[2] Kornbluh R D, Pelrine R, Joseph J, Heydt R, Pei Q and Chiba S 1999 High-field electrostriction of elastomeric polymer dielectrics for actuation *Proc. SPIE* **3669** 149–61

[3] Henke E-F M, Schlatter S and Anderson I A 2017 Soft dielectric elastomer oscillators driving bioinspired robots *Soft Robot* (https://doi.org/10.1089/soro.2017.0022)

[4] Maffli L, Rosset S, Ghilardi M, Carpi F and Shea H 2015 Ultrafast all-polymer electrically tunable silicone lenses *Adv. Funct. Mater.* **25** 1656–65

[5] Poulin A, Demir C S, Rosset S, Petrova T V and Shea H 2016 Dielectric elastomer actuator for mechanical loading of 2D cell cultures *Lab. Chip* **16** 3788–94

[6] Rosset S and Shea H R 2016 Small, fast, and tough: shrinking down integrated elastomer transducers *Appl. Phys. Rev.* **3** 031105

[7] York A, Dunn J and Seelecke S 2013 Systematic approach to development of pressure sensors using dielectric electro-active polymer membranes *Smart Mater. Struct.* **22** 094015

[8] Keplinger C, Li T, Baumgartner R, Suo Z and Bauer S 2011 Harnessing snap-through instability in soft dielectrics to achieve giant voltage-triggered deformation *Soft Matter* **8** 285–8

[9] (http://covestro.us/en/media/news-releases/2013-news-releases/2013-04-25-electroactive-polymers)-2013-Accessed 10/02/2017

[10] (http://optotune.com/products/laser-speckle-reducers)-2016-Accessed 10/02/2017

[11] Rosset S, de Saint-Aubin C, Poulin A and Shea H 2017 Assessing the degradation of compliant electrodes for soft actuators *Rev. Sci. Instrum.* **88** 105002

[12] Rosset S, Araromi O A, Schlatter S and Shea H R 2016 Fabrication process of silicone-based dielectric elastomer actuators *JoVE J. Vis. Exp.* e53423–53423

[13] Matysek M, Lotz P and Schlaak H F 2011 Lifetime investigation of dielectric elastomer stack actuators *IEEE Trans. Dielectr. Electr. Insul.* **18** 89–96

[14] Haruna M, Kubo K, Fukusumi K and Tamida T 2007 Development of soft actuator: mechanism with vibration element using dielectric elastomer to generate large displacement *Proc. SPIE* **6524** 652418

[15] Zhang M, Denes I, Xue Y and Buchmeiser M R 2016 Ageing of silicone-based dielectric elastomers prepared with varying stoichiometric imbalance: changes in network structure, mechanical, and electrical properties *Macromol. Chem. Phys.* **217** 1729–36

[16] Rosset S, Schlatter S and Shea H R 2016 Project Peta-pico-Voltron. (http://petapicovoltron.com/)

[17] Madsen F B, Zakaria S, Yu L and Skov A L 2016 Mechanical and electrical ageing effects on the long-term stretching of silicone dielectric elastomers with soft fillers *Adv. Eng. Mater.* **18** 1154–65

[18] Araromi O A, Rosset S and Shea H R 2015 Versatile fabrication of PDMS-carbon electrodes for silicone dielectric elastomer transducers transducers 2015 *2015 18th Int. Conf. on Solid-State Sensors* Actuators and Microsystems (IEEE) pp 1905–8

[19] Kujawski M, Pearse J and Smela E 2010 PDMS/graphite stretchable electrodes for dielectric elastomer actuators *Proc. SPIE* **7642** 76420R

[20] McCoul D, Hu W, Gao M, Mehta V and Pei Q 2016 Recent advances in stretchable and transparent electronic materials *Adv. Electron. Mater.* **2** 1500407

[21] O'Brien B M, Calius E P, Inamura T, Xie S Q and Anderson I A 2010 Dielectric elastomer switches for smart artificial muscles *Appl. Phys.* A **100** 385–9

[22] Rosset S and Shea H R 2012 Flexible and stretchable electrodes for dielectric elastomer actuators *Appl. Phys.* A **110** 281–307

[23] Schlatter S, Rosset S and Shea H 2017 Inkjet printing of carbon black electrodes for dielectric elastomer actuators *Proc. SPIE* **10163** 1016311

[24] Le Saux V, Marco Y, Calloch S, Doudard C and Charrier P 2010 Fast evaluation of the fatigue lifetime of elastomers based on a heat build-up protocol and micro-tomography measurements - document *Int. J. Fatigue* **32** 1582–90

[25] Brinson L C and Gates T S 1995 Effects of physical aging on long term creep of polymers and polymer matrix composites *Int. J. Solids Struct.* **6–7** 827–46

[26] Diani J, Fayolle B and Gilormini P 2009 A review on the Mullins effect *Eur. Polym. J.* **45** 601–12

[27] Ayoub G, Zaïri F, Naït-Abdelaziz M, Gloaguen J M and Kridli G 2014 A visco-hyperelastic damage model for cyclic stress-softening, hysteresis and permanent set in rubber using the network alteration theory *Int. J. Plast.* **54** 19–33

[28] Şerban D A, Marşavina L and Modler N 2015 Low-cycle fatigue behaviour of polyamides *Fatigue Fract. Eng. Mater. Struct.* **38** 1383–94

[29] Kanniah V, Forbus T R, Parker S and Grulke E A 2011 Partition coefficients for a mixture of two lubricant oligomers *J. Appl. Polym. Sci.* **122** 2915–25

[30] Lee J N, Park C and Whitesides G M 2003 Solvent compatibility of poly(dimethylsiloxane)-based microfluidic devices *Anal. Chem.* **75** 6544–54

[31] Buchberger G, Schoeftner J, Bauer S, Jakoby B and Hilber W 2013 A comparison of the electromechanical characteristics of dielectric elastomer minimum energy structures (DEMES) and planar dielectric elastomer actuators (p-DEAs) *Proc. SPIE* **8687** 86871G

[32] Bettina F, Micah H, Gianluca R and Stefan S 2017 Effect of screen printing parameters on sensor and actuator performance of dielectric elastomer (DE) membranes *Sensors and Actuators A: Physical* **265** 10–9

[33] Adrega T and Lacour S P 2010 Stretchable gold conductors embedded in PDMS and patterned by photolithography: fabrication and electromechanical characterization *J. Micromechanics Microengineering* **20** 055025

[34] Bathias C 2013 Fatigue of polymers and elastomers *Fatigue of Materials and Structures - Application to Damage and Design* ed C Bathias and A Pineau (New York: Wiley) pp 205–22